2011 IEEE/RSJ International Conference on
Intelligent Robots and Systems
September 25-30, 2011. San Francisco, CA, USA

Bio-inspired Active Soft Orthotic Device for Ankle Foot Pathologies

Yong-Lae Park, Bor-rong Chen, Diana Young, Leia Stirling,
Robert J. Wood, Eugene Goldfield, and Radhika Nagpal

Abstract— **We describe the design of an active soft ankle-foot orthotic device powered by pneumatic artificial muscles for treating gait pathologies associated with neuromuscular disorders. The design is inspired by the biological musculoskeletal system of a human foot and a lower leg, and mimics the muscle-tendon-ligament structure. A key feature of the device is that it is fabricated with flexible and soft materials that provide assistance without restricting degrees of freedom at the ankle joint. Three pneumatic artificial muscles assist dorsiflexion as well as inversion and eversion. The prototype is also equipped with various embedded sensors for gait training and gait pattern analysis. The prototype is capable of 12° dorsiflexion from a resting position of an ankle joint and a 20° dorsiflexion from plantarflexion. Results of early feedback control experiments show controllability of ankle joint angles. Ultimately, we envision a system that not only can provide physical support to improve mobility but also can increase safety and stability during walking, while enhancing muscle usage and encouraging rehabilitation.**

I. INTRODUCTION

In patients with neuromuscular disorders, such as stroke, cerebral palsy (CP), amyotrophic lateral sclerosis (ALS), and multiple sclerosis (MS), pathologies of the ankle-foot can result in abnormal gaits over time. Drop foot is one example. Due to the damage of the long nerves or of the brain/spinal cord, the anterior muscles of the lower leg, which work for dorsiflexion, become weaker while the posterior muscles become stiffer. As a result, the foot drops in swing phases causing toe strikes instead of heel strikes. It sometimes results in trip and fall. The treatment of drop foot using orthosis has the potential not only for providing immediate assistance in walking but also for preventing the development of abnormal gaits over time.

There have been different approaches to assist drop foot for decades. The most widely used solution is to wear a passive orthotic device, such as an ankle-foot orthosis (AFO) [3], [7], [22], which forces the joint angle to be close to 90°. Such passive orthoses prevent the foot from dropping during the swing phase and help the users improve their gaits. However, long-term use of this type of passive orthoses makes the user more physically dependent on the device, as the immobilization or misuse of specific muscles may induce weakness and atrophy [1], [10], [19]. Passive AFOs were not designed to help the user exercise and train the weak muscles. Additional drawbacks of long-term use are neural adaptations that gradually reduce the muscle activity over time [9]. Neural adaptation of motor representation with spinal cord injury or immobilization has been discussed in [5], [12]. Thus, passive AFOs often put a lot more pressure on physical therapy to compensate for these unwanted long term effects.

Active orthotic devices are another approach to address pathological gaits. While active devices require relatively complicated systems compared to passive braces, with appropriate control, they can provide higher independence, as seen with active prosthetic legs [6], [14], [16], [21]. Active devices can also be used to re-educate the neuro-motor system [20]. Previous work has shown the efficacy of adaptive control with active devices [4]. Several methods have been implemented to obtain active elements. Series elastic actuators (SEAs) with a rigid plastic AFO frame have been used for controlling the ankle joint angle [13]. McKibben pneumatic artificial muscle actuators with carbon fiber reinforced foot and leg frames have been implemented for supplementing weak muscles for both dorsiflexion and plantarflexion [8], [11]. McKibben muscles have been also used in a hip joint orthosis [23]. An active knee orthotic device using electrorheological fluid has been developed for providing variable damping characteristics [24]. However, the above devices all require rigid frame structures and mechanical joints, which reduce the number of inherent degrees of freedom of the joint. To avoid limiting the motion of the joint, active soft orthotic devices for knee motions without rigid frames have been developed using shape memory alloy (SMA) wires for actuation [27]. Although SMA wires showed potential to be embedded in a soft material, power management and response time turned out to be limitations for a practical use.

We present a novel active, soft orthotic device powered by pneumatic artificial muscles for use in treating gait pathologies associated with neuromuscular disorders. The current design mimics the muscle-tendon architecture in a biological musculoskeletal system of a human foot and a lower leg. In contrast to prior orthotic designs that either constrain or actuate the ankle joint only in a sagittal plane, the device has multiple pneumatic artificial muscles that mimic not only the

This work was supported by the Wyss Institute for Biologically Inspired Engineering and National Science Foundation (NSF) grant CNS 0932015. Any opinions, findings, and conclusions or recommendations expressed in this material are those of the authors and do not necessarily reflect the views of the NSF.

Y.-L. Park, D. Young, and L. Stirling are with the Wyss Institute, Harvard University, Boston, MA 02115. {ylpark, diana.young, leia.stirling}@wyss.harvard.edu

B. Chen is with the School of Engineering and Applied Science, Harvard University, Cambridge, MA 02138. brchen@eecs.harvard.edu

R. J. Wood and R. Nagpal are with Faculty of the School of Engineering and Applied Science, Harvard University, Cambridge, MA 02138, and with the Wyss Insititute, Harvard University, Boston, MA 02115. {rad, rjwood}@eecs.harvard.edu

E. Goldfield is with the Children's Hospital Boston, Boston, 02115, and with the Wyss Institute, Harvard University, Boston, MA 02115. Eugene.Goldfield@childrens.harvard.edu

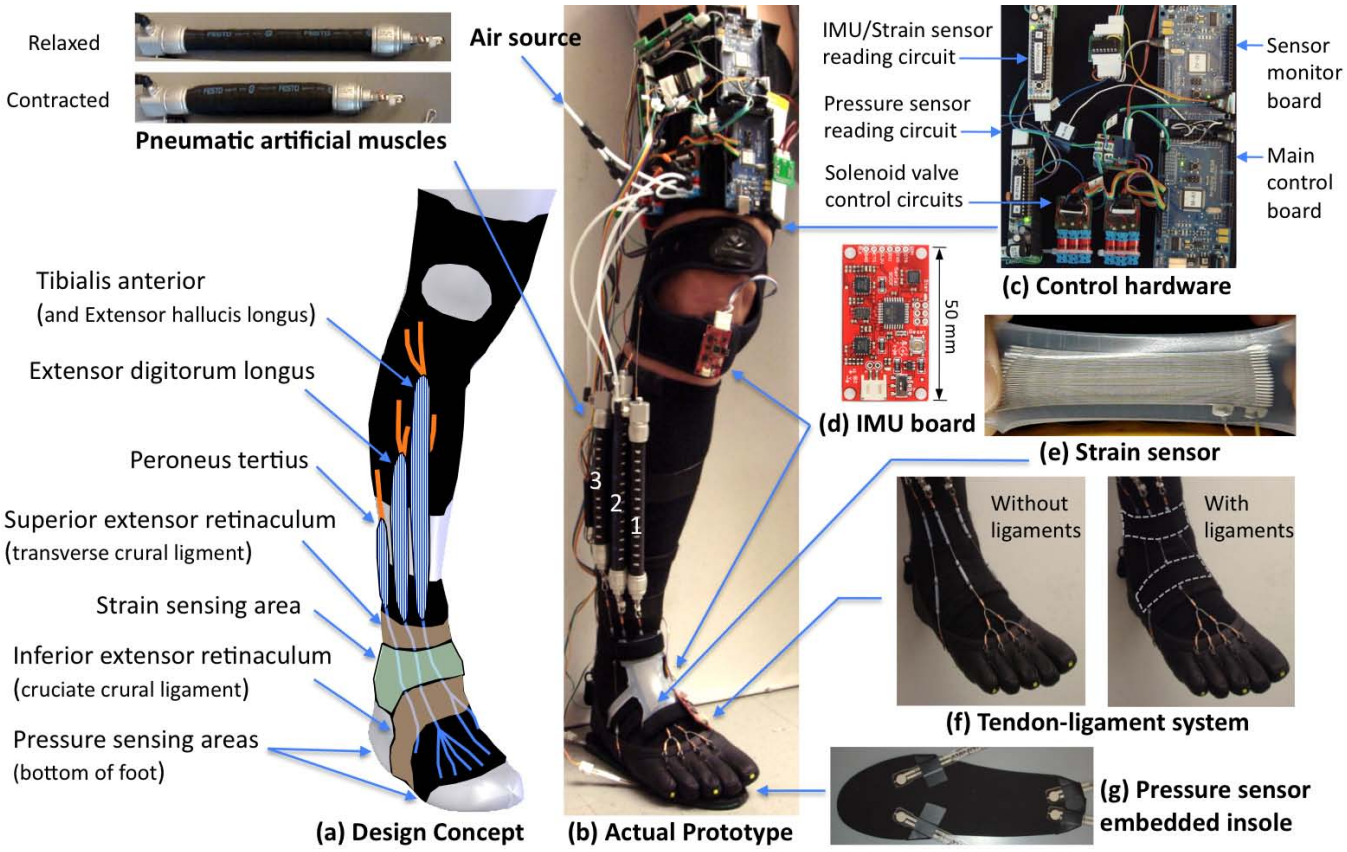

Fig. 1. Main design of the active soft orthotic device, highlighting key components.

morphology but also the functionality of the real biological muscles in terms of its ability to control varied sagittal and mediolateral ankle motions such as dorsiflexion, inversion, and eversion. The prototype is made of soft plastics and composite materials that provide a light and flexible, but relatively robust, structure. The device is also equipped with various types of sensors, such as a strain sensor, inertial measurement units (IMUs), and pressure sensors. The strain sensor and the IMUs provide information on joint angle changes, while the pressure sensors detect foot contact with the ground.

Ultimately, we envision a system that not only can provide physical support to improve mobility but also can increase safety and stability, while enhancing muscle usage and encouraging rehabilitation.

To the best of our knowledge, this is the first approach to design an active orthotic device with soft materials by mimicking the existing biological muscle-tendon system of a human body.

The rest of the article is organized as follows. Section II describes the design and fabrication of the prototype. Section III discusses the sensor validation and mechanical characterization of the system. Section IV presents the current control strategy and the results of feedback control. We conclude with a discussion of future work, which includes potential extensions of the prototype.

II. DESIGN

Figure 1(a) describes the concept of the design. The prototype can be divided into three physical layers: base, actuation, and sensing. The control hardware connects the actuation and sensing layers to provide capability for executing complex control rules. The entire prototype including electronics and batteries weighs 950 g.

A. Base Layer

The base layer contains the innermost components that make physical contact with the user's skin. This layer includes the foot and knee braces to which the actuation forces are transmitted. A commercial neoprene knee strap[1] and a five-toed leather shoe[2] were modified to be used as the knee and foot braces, respectively.

B. Actuation Layer

The actuation layer includes an artificial muscle and tendon system. Three artificial muscles are placed on the anterior part of the lower leg, with their artificial tendons anchored at the knee brace and the foot brace. Each artificial muscle was designed as a counterpart to an actual anterior muscle for dorsiflexion so that the device can provide the supplementary force to the corresponding muscle. The

[1]#419 Multi-Action Knee Strap, McDavid, Woodridge, IL 60517, USA.
[2]Performa, Vibram, Albizzate, Italy.

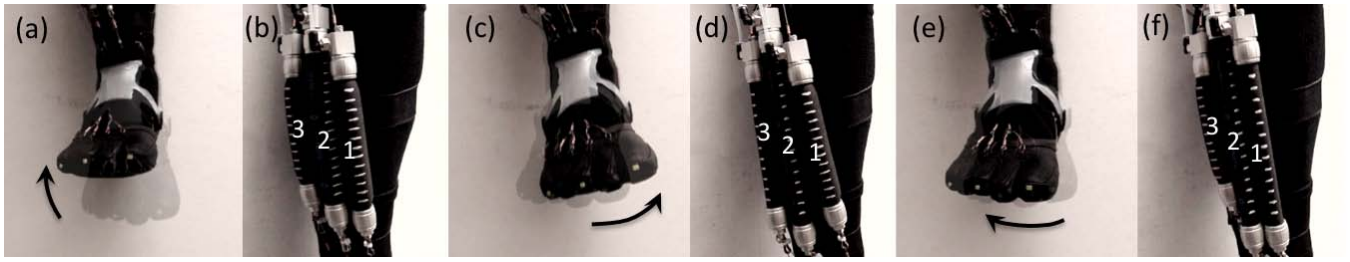

Fig. 2. Actively assisted ankle motions: (a) Dorsiflexion (b) with all three muscles actuated; (c) Inversion (d) with only muscle 1 actuated; (e) Eversion (f) with only muscle 3 actuated.

artificial tendon is located close to where the corresponding biological tendon is attached. As the artificial muscle contracts, its artificial tendon pulls the anchoring points on the foot brace resulting in dorsiflexion of the foot. Since the three muscles can be actuated independently, they can also generate mediolateral motions, such as inversion and eversion, as well as dorsiflexion, which will be useful for foot stability control during the ground contact phase of walking. Figure 2 shows possible ankle motions generated by different combinations of actuated muscles.

Figure 1(b) shows the actual prototype integrated on a subject's right leg. Three off-the-shelf pneumatic artificial muscles[3] are used for actuation, and two off-the-shelf miniature solenoid valves[4] are connected to each muscle for air injection and release. The proximal side of each muscle is anchored to the knee brace, and the distal side is anchored to the foot brace through metal tendon cables that are flexible, but inextensible. Metal hooks were firmly sewn onto the knee and foot braces to provide anchoring points for the tendon cables. The hooks make the muscles easy to attach to and detach from the braces. Since the knee brace has anchoring points only below the knee joint, the muscle-tendon system does not constrain the range of knee motion. Muscles 1 and 3 (representing the tibialis anterior and peroneous tertius) provide inversion and eversion functions, respectively, as well as dorsiflexion. Muscle 2 (representing the extensor digitorum longus) provides only dorsiflexion.

The tendon system is described in Figure 1(f). While Muscle 1 and 3 have only one anchoring point, Muscle 2 has multiple anchoring points on the foot brace. The differential tendon mechanism of Muscle 2, similar to the foot design of a wall-climbing robot [18], distributes the pulling force from one tendon cable to four anchoring points. Teflon® tubes hold the tendon cables and are sewn onto the foot brace. These tubes allow the cables to easily slide when the muscles are actuated. In addition to the teflon tubes, nylon strap ligaments constrain the movement of the tendon cables allowing the actuators to pull the foot.

The flexibility of the actuators and the other mechanical components makes the entire prototype conformable to a human leg. Also, since the supporting materials, such as rubber, neoprene, and nylon, included in the prototype are flexible and soft, the device is wearable and maintains a compact form factor.

C. Sensing Layer

The sensing layer is the outermost part of the prototype that includes all the sensors.

1) Strain Sensor: We used a custom-built strain sensor (Figure 1(e)) for measuring the ankle joint angle changes. Although there are different types of accurate commercial strain gauges, few of them are designed for measuring large strain on a flexible surface. Figure 3(a) shows the basic design of the custom-built strain sensor. Micro-channels, filled with a liquid metal alloy, Eutectic Gallium Indium (EGaIn), are embedded in a silicone rubber layer[5], as described in [25]. When the material experiences strain in the axial direction of the channels, the overall channel length increases and the cross-sectional areas of the channels decrease (Figure 3 (b)), which causes an increase in the overall resistance of the channel. Since the channels are filled with conductive liquid, the strain sensor is highly flexible and stretchable. The channel size is 250 μm x 250 μm (Figure 3 (c)), and the overall thickness of the sensor is 1.5 mm. The nominal resistance at rest is 6.3 Ω. The strain sensor was calibrated by applying axial strain up to 100% (Figure 3(d)). The gauge factor (G) of the strain sensor can be found from the following equation:

$$\frac{\Delta R}{R} = G\varepsilon + \alpha\theta \tag{1}$$

where ΔR is resistance change, R is resistance at rest, ε is applied strain, α is temperature coefficient, and θ is temperature change. Assuming there was no temperature change during the calibration, the experimental gauge factor of the strain sensor is 3.04 based on the calibration result.

2) Inertial Measurement Unit (IMU): We use two off-the-shelf 9-degree-of-freedom IMUs[6] (Figure 1(d)) to measure the orientations of the lower leg and the foot. The IMUs provide data from three types of MEMS sensors: 3D accelerometer, 3D angular rate gyroscope, and low field 3D magnetic sensors. An on-chip sensor fusion algorithm derives the 3D orientation of the IMU circuit board using the sensor inputs. Using two IMUs, mounted on the foot and lower

[3]DMSP-10-120(140, 160)-RM-CM, Festo, Esslingen, Germany.
[4]NEX-2-03-L, Parker Hannifin Corp., Cleveland, OH 44124, USA.
[5]EcoFlex0030, Smooth-On, Inc., Easton, PA 18042, USA.
[6]SEN-09623, 9DOF Razor IMU, Sparkfun Electronics, Boulder, CO 80301, USA.

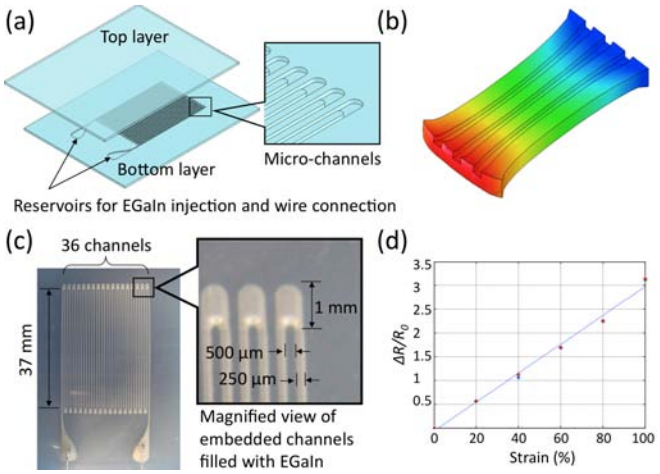

Fig. 3. (a) Strain sensor design. (b) Finite element analysis of an elastomer sample that experiences longitudinal stain resulting in the dimension changes of the embedded channels. (Color change represents displacement.) (c) Actual strain sensor prototype with dimensions. (d) Calibration result showing linear response.

leg, we compute the ankle joint angle by differencing the orientation vectors of the two IMUs.

3) Pressure Sensor: Foot pressure sensing is necessary to identify the foot ground contacts, and gait cycle events. Although the strain sensors and IMUs provide the information on the ankle joint angle, they are not sufficient to detect the ground contacts of the foot. The pressure sensors are embedded in a shoe insole to determine which part of the foot is in contact to the ground in real-time. Four off-the-shelf force sensitive resistor sensors[7] are embedded in the insole (Figure 1(g)). While the current pressure sensors are used as on-off switches in the current prototype, they can be replaced with more accurate sensors, such as [25], that can read actual foot pressures.

D. Control Hardware

All of the electronics (control hardware) including batteries are attached to a neoprene thigh brace [8] (Figure 1(c)). The control hardware contains multiple micro-controller units (MCUs) to support tasks divided into four major stages: sensing, signal processing, control, and actuation (Figure 4).

At the sensing stage, all the sensors are sampled at 50 Hz. Each type of sensors has its own MCU to sample independently. After samples are acquired, different processing algorithms for each sensor type are applied in the signal processing stage. We chose Atmega328P[9], an off-the-shelf micro-controller, as the MCU for sensor sampling and signal processing. Also, each IMU has its own MCU to run a direct-cosine-matrix (DCM)-based orientation estimation algorithm similar to the one described in [2]. Each IMU board computes a 3D orientation vector and sends the value to the IMU master board using standard serial protocol (UART).

[7]FlexiForce-A201-25lb, Tekscan Inc., Boston, MA 02127, USA.
[8]#473 Thigh Sleeve, McDavid, Woodridge, IL 60517, USA.
[9]Atmel, San Jose, CA 95131, USA.

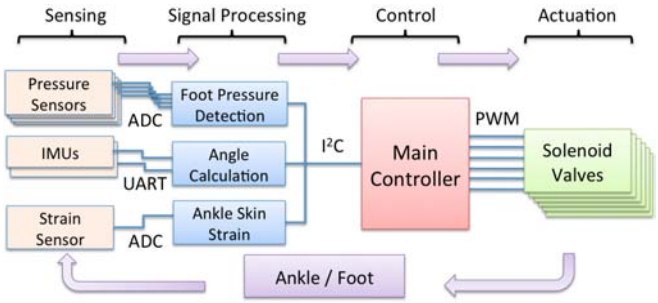

Fig. 4. Control system architecture.

Then, the IMU master MCU determines the joint-angle by computing the angle between the two orientation vectors. The pressure sensing MCU produces an on-off output for each pressure sensor. The strain sensor MCU simply records the analog readings from the strain sensor analog circuit. Although the MCUs for the pressure and strain sensors currently do not perform significant processing, they are reserved for future implementation of more sophisticated filtering algorithms.

The control stage contains one dedicated Atmega1280 MCU. This main control MCU has access to all sensor data. To transmit the sensor data in real time, an I^2C bus is shared among all sensor MCUs and the main control MCU, which runs a control loop at 50 Hz for actuation.

The actuation stage carries out commands to the pneumatic muscles generated at the control stage by signaling the solenoid valves connected to the pneumatic muscles. Pulse-width-modulation (PWM) signals are used to control the air flow through the solenoid valves.

III. Characterization

The prototype was characterized in two main functional categories: sensing and actuation. In addition, power consumption is briefly discussed at the end of this section. All the testing for characterization was done with the primary author as a subject, and the testing procedure was reviewed by Harvard Medical School (HMS) Committee on Human Studies.

A. Sensor Validation

All three types of sensors were characterized. The accuracy of the strain sensor and IMUs were evaluated using a commercial goniometer[10], an optical angle sensor. The pressure sensors were tested to determine the threshold of a ground contact of the foot.

1) Ankle Joint Angle Sensing: The sensor system of the prototype can provide real-time information on ankle joint angle. We use the strain sensor as a reliable source of joint angle information. However, each time a user wears the orthosis, the strain sensor requires calibration. We use IMUs for calibrating the strain sensor by establishing a linear

[10]PASPORT Goniometer Sensor PS-2137, PASCO, Roseville, CA 95747, USA.

mapping between strain sensor readings and joint angles measured by IMUs.

We conducted a validation experiment of the strain sensor and the IMUs with the goniometer used as ground truth for the ankle joint angle. As shown in Figure 5(a), we attached two IMUs to the goniometer that is mounted to the right foot of the subject. The strain sensor was firmly attached to the front side of the ankle joint. Once all the sensors were mounted, the subject freely moved the ankle in plantarflexion and dorsiflexion for 20 minutes. Figure 5(b) shows a 30 second segment from the validation experiment. The data show that both the strain sensor and IMUs provide accurate joint angle measurements during the experiment. For the IMU, the mean error was $0.135 \pm 2.85°$. For the strain derived angle, the mean error was $0.255 \pm 1.63°$.

2) Foot Pressure Sensing: We characterized the FSR pressure sensors in order to choose a threshold for determining when the foot is on the ground. With no load, the resistance of the FSR pressure sensors are at or above 1 MΩ. With a 143 *lb* adult standing on the foot insole, the resistance consistently lowers to below 500 kΩ. Thus, we selected 800 kΩ as the threshold for detecting foot contact from our device. We expect this threshold to work in most cases, but it is also easily tunable for different users.

B. Actuation System Characterization

The mechanical system was characterized to show the response time, the linearity of the actuators, and the repeatability of feed-forward control. The prototype was assembled on the subject's right leg (Figure 1(b)). The subject sat on a rigid bench hanging the foot in the air. The subject was able to move the lower leg and the foot without any constraint.

Due to the non-linearity of pneumatic muscles, the proportional control of pneumatic muscles is not as straightforward as linear actuators, such as DC motors. Using proportional valves that control the input air pressure of the muscles by changing input voltage is one way for proportional control [26]. Another method is using PWM control with binary on/off solenoid valves [17], [15]. We employed the PWM method due to the compact form factor of the binary valves. All the experiments were done using lab-bench air supply. The source air pressure was 100 psi with a flow rate of 0.4 scfm during the experiments.

By changing the duty-cycle of the PWM controller, we achieved different contraction and release speeds of the pneumatic muscles. The following four experiments were carried out to characterize the mechanical system.

1) Full contraction from a resting position and full release to the resting position with different speeds (different PWM duty-cycles).
2) Full contraction and release cycles with forced plantarflexion by a drop-foot simulator.
3) Repetition of contraction-hold-release cycles with different muscle contraction speeds.
4) Incremental contractions (repetition of contraction and hold cycles) with different contraction speeds.

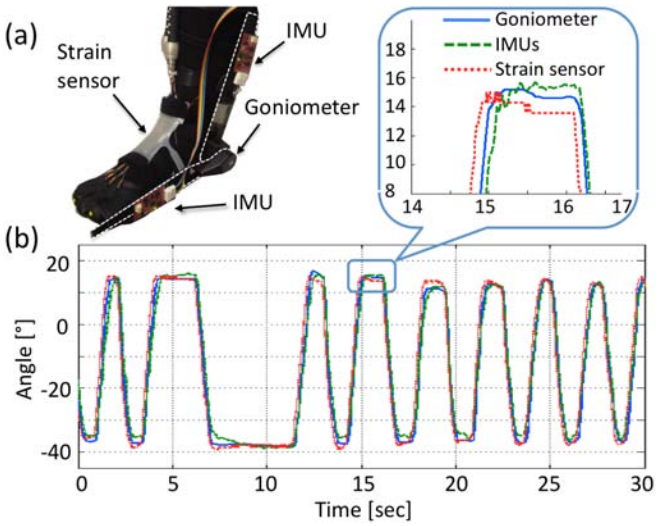

Fig. 5. Sensor validation experiments. (a) Experimental setup with a strain sensor, two IMUs, and a goniometer. (b) Sensor validation result with ankle joint angle measurement.

All of the above experiments except Experiment 2 started with a resting position of the foot. The subject's resting ankle joint angle varied slightly between trials but was approximately -11°. Experiment 1 verified that the muscle contraction speed can be controlled by PWM duty-cycles (Figure 6(a)). The limiting factors of the contraction speed are flow rate of the air source and valve response time. The expriment also showed the maximum change in ankle dorsiflexion was approximately 12°.

Experiment 2 demonstrated the maximum dorsiflexion range can be increased if the foot was forced to a plantarflexion position (Figure 6(b)). An elastic band was attached to the subject's heel to plantarflex the foot further than the subject's standard resting position to simulate over-stiff posterior muscles, which can cause drop-foot (Figure 6(c)). In this case, the resting position of the foot was -22°. The maximum angle change from a forced plantarflexion position was approximately 20°.

The feed-forward control (Experiments 3 and 4) results show that intermediate joint angles can be achieved by specifying the contraction time (Figure 6(d) and 6(e)). Although intermediate angles were achieved repeatedly with feed-forward control, the achieved angles gradually changed during the holding phase due to air leakage of the solenoid valves. Thus feedback control is necessary for more accurate joint angle control.

C. Power Consumption

Since the main actuation is pneumatically powered, the electric power consumption of the prototype is relatively small. Three rechargeable polymer lithium-ion batteries[11] are able to provide enough power to operate the entire system for more than two hours. The whole control hardware, excluding

[11] 3.7V–900mAh, Sparkfun Electronics, Boulder, CO 80301, USA.

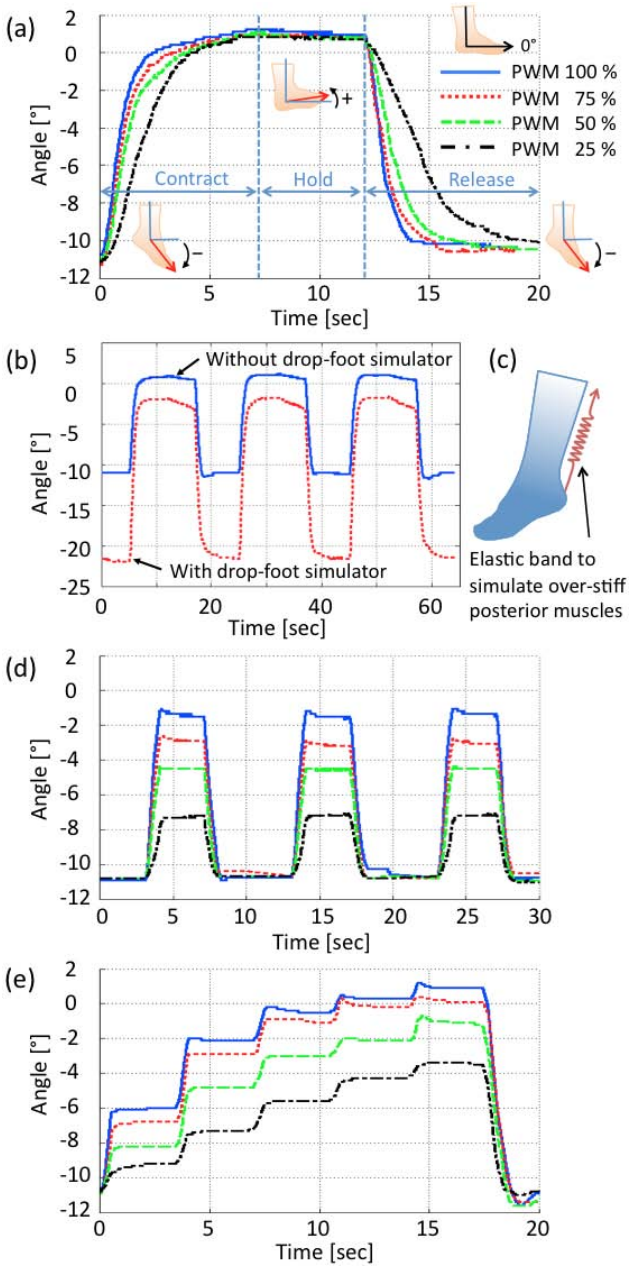

Fig. 6. Mechanical characterization results. (a) Experiment 1: full muscle contractions and releases with different PWM duty-cycles. (b) Experiment 2: Dorsiflexion range comparison between a resting position and a forced plantarflexion position. (c) Drop-foot simulator with an elastic band attached to the subject's heel to force plantarflexion. (d) Experiment 3: repeated contractions (e) Experiment 4: incremental contractions.

the solenoid valves, requires 2.5 W, and the valve circuits require 1.5 W on average.

IV. CONTROL

Due to the highly nonlinear properties of the mechanical system and a human body that directly makes physical interactions with the device, it is very difficult to construct an analytical model of the entire system. Therefore, we decided to implement simple controllers with experimental tuning as

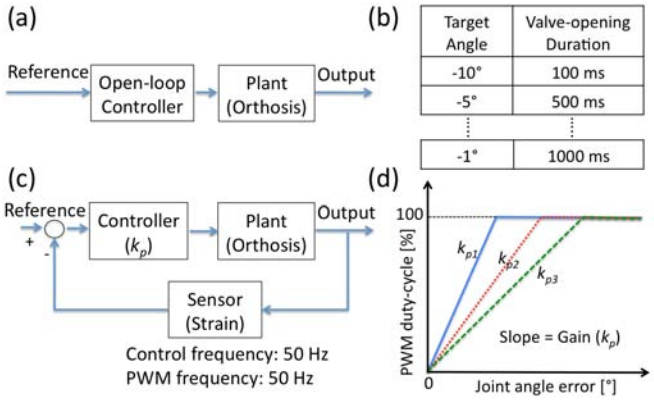

Fig. 7. Basic controllers to achieve target joint angles. (a) Feed-forward controller. (b) Example of a look-up table for feed-forward control with PWM duty-cycle=100%. (c) Feedback P controller. (d) k_p selection plot ($k_{p1} > k_{p2} > k_{p3}$).

an initial step for control instead of finding complicated models of the system. Two basic controllers were tested: a feed-forward controller and a feedback proportional (P) controller (Figure 7). In the feed-forward controller, as briefly discussed in Section III-B, the proportional muscle contraction is achieved by opening the solenoid valves for a specified time in order to reach a target angle. The duration of valve opening is computed from a model derived from the mechanical characterization shown in Figure 6(a). Figure 7(b) shows an example look-up table for valve opening times based on the characterization result with the 100% PWM duty-cycle.

The P controller contains a feedback loop operating at 50 Hz that reads the strain sensor values and dynamically sets the commands to contract or release the artificial muscles (by opening or closing the valves). As depicted in Figure 7(c), the control loop is tuned by the proportional gain, k_p, which is the ratio of PWM duty-cycle to joint angle error (Figure 7(d)). Although the duty-cycle increases as the error increases with a proportion of k_p, it cannot exceed 100% due to the nature of PWM control. The choice of k_p impacts the settling time, overshoot, and steady state error. The PWM duty-cycle is determined by the following rules:

$$d_c = \begin{cases} -e \cdot k_p & \text{if } e < 0 \\ 0 & \text{otherwise,} \end{cases} \quad d_r = \begin{cases} e \cdot k_p & \text{if } e > 0 \\ 0 & \text{otherwise} \end{cases}$$

where d_c and d_r are duty-cycles for muscle contraction and release, respectively, and e is joint angle error.

In our control experiments, k_p was varied to achieve two target angles, -5° and -2°. Figure 8 shows examples of step responses of the controller with three different k_p values: 50, 250, and 1000. The best performance, i.e., lowest settling time and steady state error, was achieved with a k_p of 250 for both target angles. Figure 9 summarizes the performance of the controller with different k_p values.

The performance of the feed-forward and feedback controllers are compared in Figure 10(a). Although both controllers were able to achieve the target angles repeatedly, the feed-forward controller was not able to maintain the target

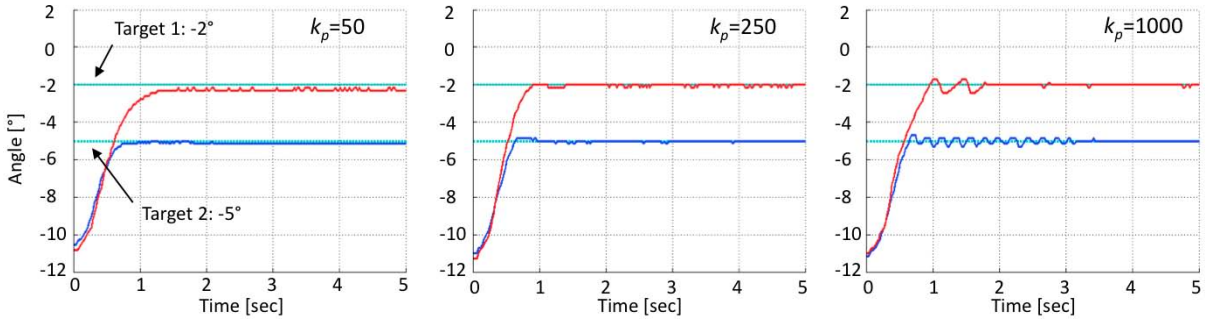

Fig. 8. Step responses of the feedback proportional controllers with different gain values: k_p=50, 250, and 1000. Two target angles (-2° and -5°) were achieved. While response times and steady state errors decrease as k_p increases, the system starts oscillating if k_p is too high.

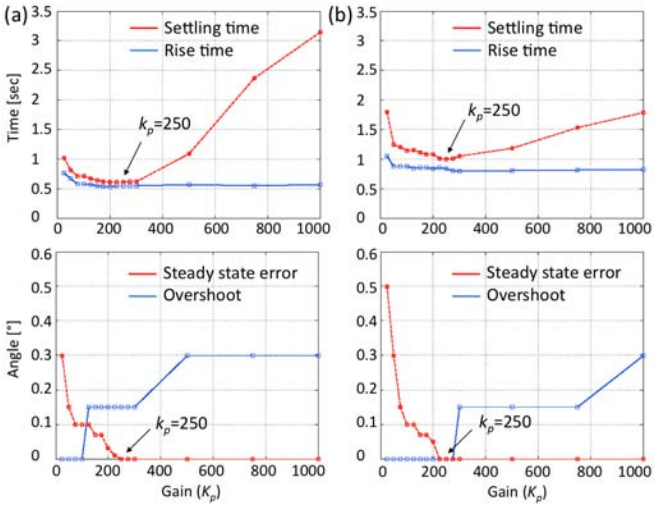

Fig. 9. Feedback controller performance with different proportional gain (k_p) values and target angles. (a) Target angle: -5°. (b) Target angle: -2°.

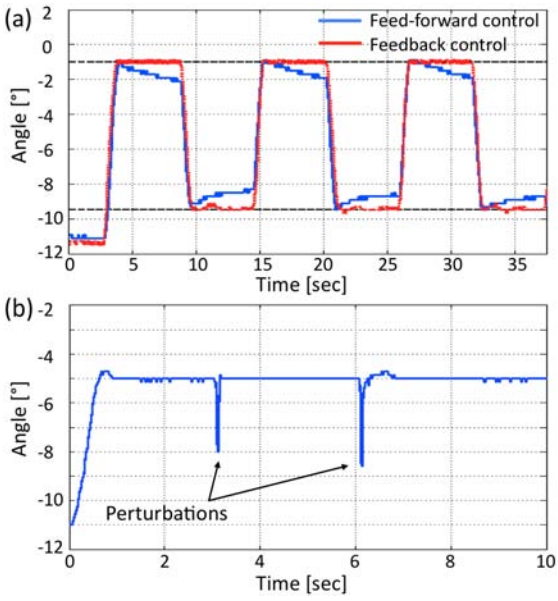

Fig. 10. Set-point tracking performance. (a) Feed-forward and feedback controller comparison following two target angles (-2° and -9.5°) repeatedly. (b) Perturbation rejection with k_p=250 and target angle=−5°.

angles over a period of time due to air leakage of the valves, while the feedback controller proved the ability to track the set-point target angle. The capability of perturbation rejection was also tested (Figure 10(b)) to determine the upper limit of the gait control speed. While the system was tracking the set-point of -5°, a weight of 200 g was dropped on the toes of the subject multiple times. The perturbation was instantaneous, and the system was able to recover the original set-point angle in less than 500 ms.

V. DISCUSSION AND FUTURE WORK

The main contribution of this paper is the design and implementation of a soft active orthotic device that mimics the biological muscle-tendon architecture. The current design shows that such an orthotic device can provide active assistance without limiting 3D motion of the foot. The responses of the device when applying simple feed-forward and feedback controllers were also demonstrated. The current prototype demonstrates full integration of sensing, actuation, and power to create a nearly untethered system.

Although the current design consists of multiple physical layers to be worn, it can be easily refined to improve the wearability and to significantly reduce the form factor of the electronics in the future. The mechanical design of the device was mainly motivated by drop-foot condition. Therefore, the current design contains only three anterior muscles for assisting dorsiflexion to alleviate the drop-foot condition. However, the design principles, system architecture, and control strategies developed in this device can be readily applied to future versions with additional artificial muscles such as posterior muscles for a complete gait cycle by actively assisting plantarflexion.

While the system consumes very little power and could run on batteries for several hours, it still relies on air source connection for the pneumatic muscles. Thus, one immediate area of future work is to investigating solutions that allow complete untethered operation. Available options include portable air compressors and compressed air canisters. For the long-term success of such orthotic devices, we are also investigating relevant clinical requirements and potential control strategies that would work seamlessly with the user's motion. Our goal is to achieve a fully untethered

wearable system to provide a new level of mobility and active assistance. This will open a rich space for future rehabilitation techniques both inside and outside of the clinic.

Although the first set of experimental data presented in this paper focuses only on seated dorsiflexion and single-input single-output (SISO) control, the current device provides future opportunities for more complex control strategies. Our intention in the experiments is to demonstrate the controllability of the device rather than exploring the entire space of potential controllers. It is expected that more sophisticated control strategies will be necessary when the device is used to perform complex tasks such as active gait assistance. For example, a cooperative controller could be designed to achieve more natural ankle joint motions when controlling individual muscles. In addition, for a trajectory following task, it may be useful to pre-actuate the artificial muscles to reduce the control latencies. Another possible strategy is to implement a supervised learning algorithm to allow the device to assist the user more dynamically without overpowering the natural muscles. This would require the system to learn the user's motion patterns and calculate correct timings to provide timely actuation in order to seamlessly assist the user's intended motions.

Finally, in addition to the active assistance for walking, the device also has a significant meaning for physical therapy. Since the device is easily programmable not only for recording the ankle motions using the strain sensor but also for replaying the recorded motions, it will be highly useful for both in-clinic and in-home therapy.

VI. CONCLUSIONS

A bio-inspired active soft orthotic device was designed and prototyped using soft actuators and sensors. The prototype showed the capability of 12° and 20° of dorsiflexions from a resting foot position and from a forced plantarflexion position, respectively. The prototype also demonstrated repeatability of feed forward-control and capability of feedback control for the ankle joint angle. We believe that this bio-inspired mechanical design, constructed with entirely soft materials, will open a rich space for future rehabilitation techniques for ankle-foot pathologies.

ACKNOWLEDGMENTS

The authors would like to thank James Niemi for his support and feedback in this research. We also thank Dr. Chandana Paul for her suggestions and inputs to this project.

REFERENCES

[1] H.-J. Appell. Muscular atrophy following immobilisation: A review. *Sports Med.*, 10(1):42–58, 1990.

[2] E. R. Bachmann, I. Duman, U. Y. Usta, R. B. McGhee, X. P. Yun, and M. J. Zyda. Orientation tracking for humans and robots using inertial sensors. In *Proc. IEEE Int. Symp. Comput. Intel. Rob. Autom*, pages 187–194, 1999.

[3] S. Blanton, S. P. Grissom, and L. Riolo. Use of a static adjustable ankle-foot orthosis following tibial nerve block to reduce plantarflexion contracture in an individual with brain injury. *Phys. Ther.*, 82(11):1087–1097, 2002.

[4] J. A. Blaya and H. Herr. Adaptive control of a variable-impedance ankle-foot orthosis to assist drop-foot gait. *IEEE Trans. Neural Syst. Rehabil. Eng.*, 12(1):24–31, 2004.

[5] M. Bruelmeier, V. Dietz, K. L. Leenders, U. Roelcke, J. Missimer, and A. Curt. How does the human brain deal with a spinal cord injury? *Eur. J. Neurosci.*, 10(12):3918–3922, 1998.

[6] H. Dietl and H. Bargehr. The application of electronics in prosthetics for lower extremities (Der einsatz von elektronik bei prothesen zur versorgung der unteren extremitat). *Med. Orthop. Tech.*, 117:31–35, 1997.

[7] M. C. Faustini, R. R. Neptune, R. H. Crawford, and S. J. Stanhope. Manufacture of passive dynamic ankle-foot orthosis using selective laser sintering. *IEEE Trans. Biomed. Eng.*, 55(2):784–790, 2008.

[8] D. P. Ferris, J. M. Czerniecki, and B. Hannaford. An ankle-foot orthosis powered by artificial peumatic muscles. *J. Appl. Biomech.*, 21:189–197, 2005.

[9] J. F. Geboers, M. R. Drost, F. Spaans, H. Kuipers, and H. A. Seelen. Immediate and long-term effects of ankle-foot orthosis on muscle activity during walking: A randomized study of patients with unilateral foot drop. *Arch. of Phys. Med. Rehabil.*, 83:240–245, 2002.

[10] J. F. Geboers, J. H. van Tuijl, H. A. Seelen, and M. R. Drost. Effect of immobilization on ankle dorsiflextion strength. *Scand. J. Rehabil. Med.*, 32:66–71, 2000.

[11] K. E. Gordon, G. S. Sawicki, and D. P. Ferris. Mechanical performance of artificial pneumatic muscles to power an ankle-foot orthosis. *J. Biomech.*, 39:1832–1841, 2006.

[12] J. B. Green, E. Sora, Y. Bialy, A. Ricamato, and R. W. Thatcher. Cortical sensorimotor reorganization after spinal cord injury: an electroencephalographic study. *Neurol.*, 50(4):1115–1121, 1998.

[13] H. M. Herr and R. D. Kornbluh. New horizons for orthotic and prosthetic technology: artificial muscle for ambulation. In *Proc. of SPIE*, volume 5385, pages 1–9, 2004.

[14] H. M. Herr and A. Wilkenfeld. User-adaptive control fo a magnetorheological prosthetic knee. *Ind. Rob. Int. J.*, 30(1):42–55, 2003.

[15] S. Jien, S. Hirai, Y. Ogawa, M. Ito, and K. Honda. Pressure control valve for mckibben artificial muscle actuators with miniaturized unconstrained pneumatic on/off valves. In *Proc. IEEE/ASME Int. Conf. Adv. Intell. Mechatron.*, pages 1383–1388, 2009.

[16] J. Kastner, R. Nimmervoll, and I. P. Wagner. What are the benefits of the Otto Bock C-leg? A comparative gait analysis of C-leg, 3R45 and 3R80 (Was kann das C-leg?-Ganganalytischer vergleigh von C-leg, 3R45 and 3R80). *Med. Orthop. Tech.*, 119:131–137, 1999.

[17] T. Kerscher, J. M. Zoellner, R. Dillmann, A. Stella, and G. Caporaletti. Model and control of joints driven by fluidic muscles with the help of advanced automatic algorithm generation software. *6th Int. Conf. Climbing Walking Rob. Support Tech. Mobile Mach.*, 4:245–252, 2006.

[18] S. Kim, M. S. Spenko, S. Trujillo, B. Heyneman, D. Santos, and M. R. Cutkosky. Smooth vertical surface climbing with directional adhesion. *IEEE Trans. Rob.*, 24(1):65–74, 2008.

[19] I. Kjeken, G. Mϕller, and T. K. Kvien. Use of commercially produced elastic wrist orthoses in chronic arthritis: A controlled study. *Arthritis Rheum.*, 8(2):108–113, 1995.

[20] H. Krebs, N. Hogan, W. Durfee, and H. Herr. Rehabilitation robotics, orthotics, and prosthetics; chapter 48. *Textbook of Neural Repair and Rehabilitation (M. E. Selzer, S. Clarke, L. G. Cohen, P. W. Duncan, and F. H. Gage), Cambridge University Press*, 2005.

[21] B. G. A. Lambrecht and H. Kazerooni. Design of a semi-active knee prosthesis. In *Proc. IEEE Int. Conf. Rob. Autom.*, pages 639–645, 2009.

[22] F. Miller. *Cerebral Palsy*. Springer, 1st edition, January 2005.

[23] B. G. Nascimento, C. B. S. Vimieiro, D. A. P. Nagem, and M. Pinotti. Hip orthosis powered by pneumatic artificial muscle: Voluntary activation in absence of myoelectrical signal. *Artif. Organs*, 32(3):317–322, 2008.

[24] J. Nikitczuk, B. Weinberg, P. K. Canavan, and C. Mavroidis. Active knee rehabilitation orthotic device with variable damping characteristics implemented via an electrorheological fluid. *IEEE/ASME Trans. Mechatron.*, 15(6):952–960, 2010.

[25] Y.-L. Park, C. Majidi, R. Kramer, P. Berard, and R. J. Wood. Hyperelastic pressure sensing with a liquid-embedded elastomer. *J. Micromech. Microeng.*, 20(12), 2010.

[26] D. Shin, I. Sardellitti, Y.-L. Park, O. Khatib, and M. Cutkosky. Design and control of a bio-inspired human-friendly robot. *Int. J. Rob. Res.*, 29(5):571–584, 2010.

[27] L. Stirling, C. Yu, J. Miller, R. J. Wood, E. Goldfield, and R. Nagpal. Applicability of shape memory alloy wire for an active, soft orthotic. *J. Mater. Eng. Perform.*, 20(4-5):658–662, 2011.